Proceedings of the
Annual Stability Conference
Structural Stability Research Council
Orlando, Florida, April 12-15, 2016

Stability Considerations for the Construction of Steel I-Girder Bridges using the Incremental Launching Method

Maria E. Ponton[1], Andres F. Robalino[2], Telmo Andres Sanchez[3]

Abstract
The incremental launching method (ILM) is commonly used for bridges where erection procedures cannot be conducted from below the superstructure. In this method, the steel components are assembled on one side of the obstacle and moved longitudinally to the other supports. Deep valleys with steep slopes and environmentally sensitive areas are examples where the use of the ILM is justified. During the launching operation, the bridge I-girders cantilever out from their initial position and may be prone to stability related problems such as global lateral-torsional buckling of the system, as well as high strength demands at the cantilever support. This paper presents studies of the behavior of a three-span steel I-girder bridge consisting of four parallel girders erected with the ILM. Critical construction stages are investigated to determine the structural responses according to the AASHTO LRFD Bridge Design Specifications. These results are compared to the responses obtained from refined three-dimensional finite element models (FEM) to verify the applicability of current design methodologies for bridges erected with the ILM. In particular, analyses are conducted to assess the validity of the construction checks in the AASHTO Specifications of girders in cantilever and of systems potentially subjected to global lateral-torsional buckling. Based on the results of the studies, recommendations are provided to conduct a stability assessment of bridges erected by applying this method.

Notation

b_{fc} = full width of the compression flange
b_{ft} = full width of the tension flange
C_b = moment gradient modifier
D = web depth
E = modulus of elasticity of steel
f_{bu} = flange major axis bending stress
f_ℓ = flange lateral bending stress
F_{crw} = nominal web bend-buckling resistance for webs

[1] Junior Structural Engineer, ADSTREN, <mponton@adstren.com>
[2] Junior Structural Engineer, ADSTREN, <arobalino@adstren.com >
[3] Assistant Professor, Universidad San Francisco de Quito, <tsanchez@usfq.edu.ec>

F_{nc} = nominal flexural resistance of the compression flange

F_{yc} = compression flange yield strength

F_{yf} = flange yielding strength

F_{yt} = tension flange yield strength

F_{yw} = web yield strength

h_o = distance between flange centroids

I_{eff} = effective moment of inertia

I_x = moment of inertia with respect to the horizontal principal axis

I_{yc} = moment of inertia of the compression flange

J = torsional constant

L_g = cantilever length

M_{gl} = elastic global lateral-torsional buckling strength

M_{u_gl} = required strength for global lateral-torsional buckling

S = girder spacing

R_h = hybrid factor

R_{nc} = nominal web crippling strength

R_{ny} = nominal web yielding strength

R_u = factored concentrated load or bearing reaction

t_{fc} = thinckness of the compression flange

t_{ft} = thinckness of the tension flange

t_w = web thickness

V_{cr} = shear-buckling resistance

V_n = nominal shear resistance

V_u = shear in the web at the section under consideration due to factored loads

ϕ_b = resistance factor for bearing

ϕ_f = resistance factor for flexure

ϕ_v = resistance factor for shear

1. Introduction

The incremental launching method (ILM) is a technique in which a bridge structure is assembled behind an end support and then it is pushed to cross over an obstacle, passing by the intermediate piers until it reaches the other end. This methodology is commonly used in the construction of concrete structures, especially post-tensioned box girder bridges. Also, its implementation in steel bridges has gained popularity due its versatility. When proper considerations are taken, the steel erection with ILM can be safer, faster, and more cost-effective than other methods. The assembly of the structure on a firm surface is an advantage that reduces the possibilities of accidents and normally, requires less crane capacities than other erection schemes. Similarly, the construction

time is usually short since the launching operation is almost continuous, from the moment that the structure starts moving longitudinally, until it reaches the end support.

This paper presents the studies conducted in a typical steel I-girder bridge to highlight structural aspects that may be considered during early design phases. Contrary to other erection methods, bridges constructed with ILM are subject to a combination of structural responses that require attention during design.

2. Description of the Case Study

The Maresa Bridge is a 195.0m long structure with three equal spans that accommodates five lanes: four for motorized traffic and one for bicycles. It is located in Quito, Ecuador, and it is part of a new highway that connects two densely populated parts of the city. Figure 1 shows an elevation view, the bridge cross-section, and the geometry of a typical girder. To facilitate the construction, the bridge is divided in two structures of four and five girders named Structures 1 and 2, respectively. The composite superstructure consists of I-girders connected with inverted "V" type cross-frames, topped with a 20cm thick reinforced concrete deck. The superstructure is made of ASTM A588 Gr.50 steel and is supported by typical reinforced concrete abutments at the ends and two equal intermediate piers with cell-type sections of an approximate 35m height. The exterior supports are abutments designed to resist the vertical, transverse, and longitudinal forces that are transferred from the composite superstructure.

During the design phase, two options were considered to erect the superstructure. In the first one, provisional erection towers would be placed at approximately the third points of each span. Then, cranes located at the road level and on the sloped terrain would manipulate the girder segments to support them on the provisional towers and the substructure. The last step would be to make the field connections and remove the towers. This method, however, has two major disadvantages: Firstly, large crane capacities are needed to manipulate heavy girder segments at more than 30m of height. Secondly, this method requires the construction of provisional structures that would not be used after the bridge is erected.

The other option was to use the ILM by assembling the entire steel structures behind Abutment "B", where there is enough space to maneuver and conduct all field operations. This method proved to be safer and more cost-effective than the previous. Some of the benefits of the ILM are that all operations are conducted on firm soil, there is no need to locate any construction items in the sloped terrain, and it is significantly faster than the other method. For these reasons, the ILM was selected for the construction of this structure, and specific design features were implemented in the steel structure geometry to facilitate the launching process. LaViolette et al (2007) present a thorough discussion of particular aspects that need to be considered for successfully implementing ILM in steel girder bridges. These recommendations were considered in the design of the Maresa Bridge.

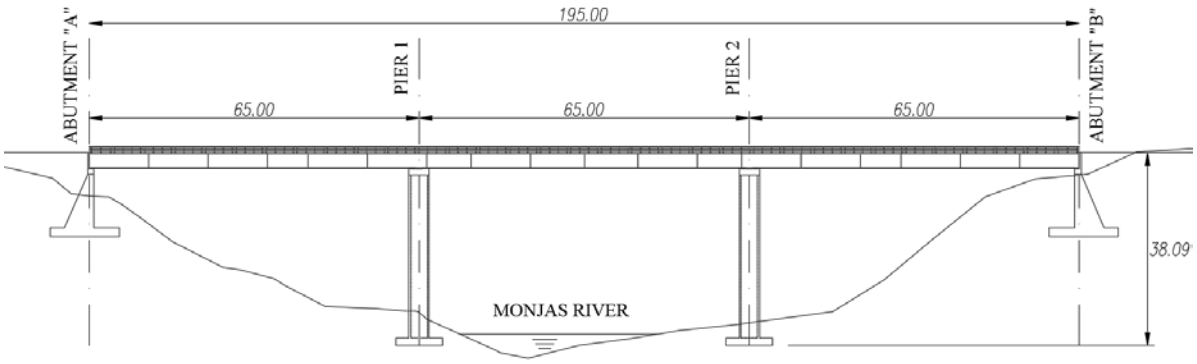

a) Elevation view

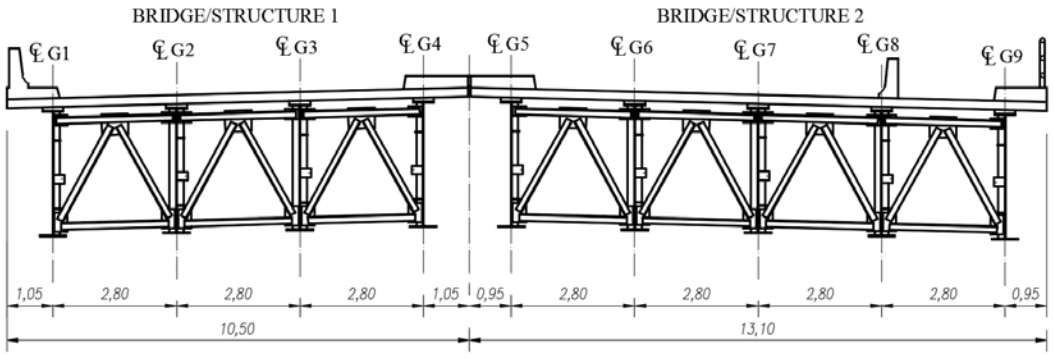

b) Superstructure cross-section

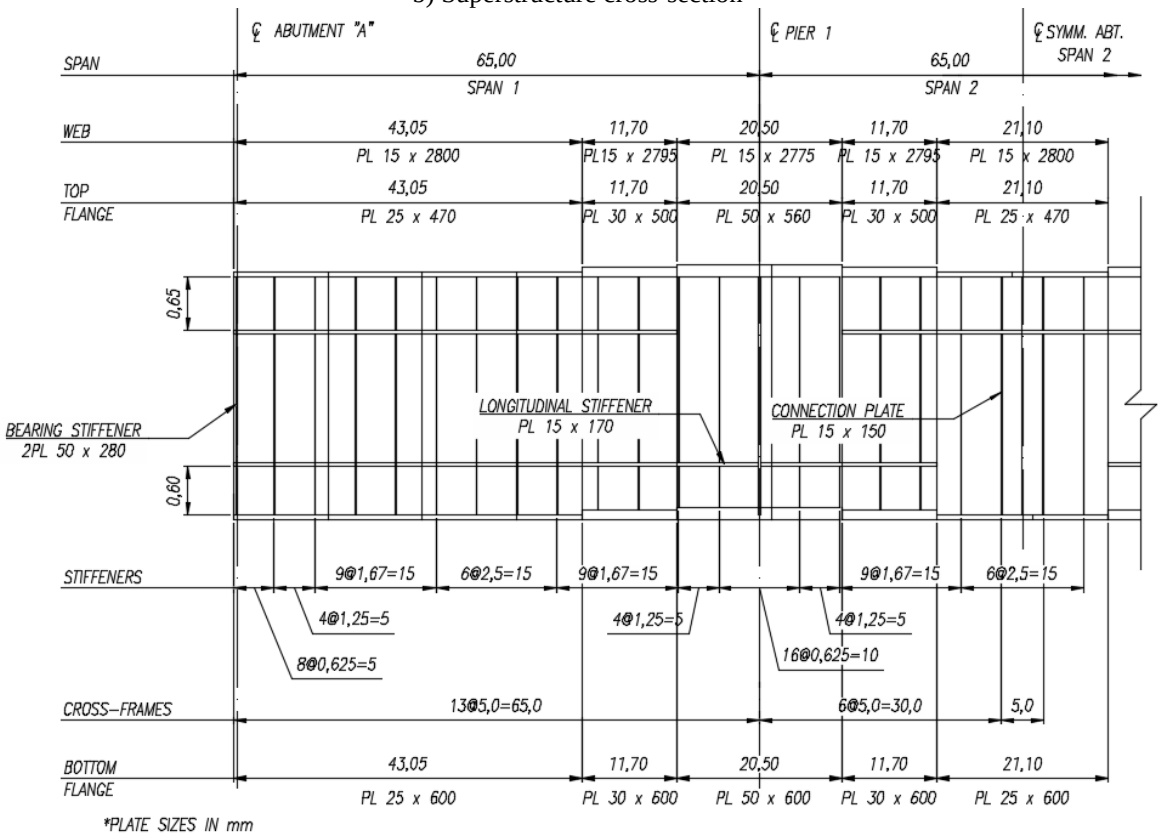

c) Girder elevation

Figure 1: General dimensions and superstructure details of the Maresa Bridge
(all dimensions in meters unless noted otherwise)

In this paper, only Structure 1, which has four girders, is studied to observe the structural stability aspects of a bridge constructed with ILM. The launching sequence is shown in Figure 2. For the field assembly behind Abutment "B", temporal supports are constructed every 50m approximately, providing five contact points along the length of each girder. These supports have a Teflon pad that facilitates the sliding of the structure while it is being launched. Strand jacks are installed in the abutment to pull the structure, then it slides over pivot bearings mounted at the abutments and the piers. Also, a launching nose is installed at the end of the steel structure to facilitate the operations. As launching progresses, the girders deflect downward in the cantilever. The nose, with its tapered shape, compensates these deflections so that its tip is not under the level of the bearings mounted on the piers and abutments. In addition, the nose reduces the cantilever length in the girders to a maximum of the span length minus the nose length. As a result, the girder stresses and deflections are considerably reduced, as compared to the values obtained if the bridge is launched without a nose.

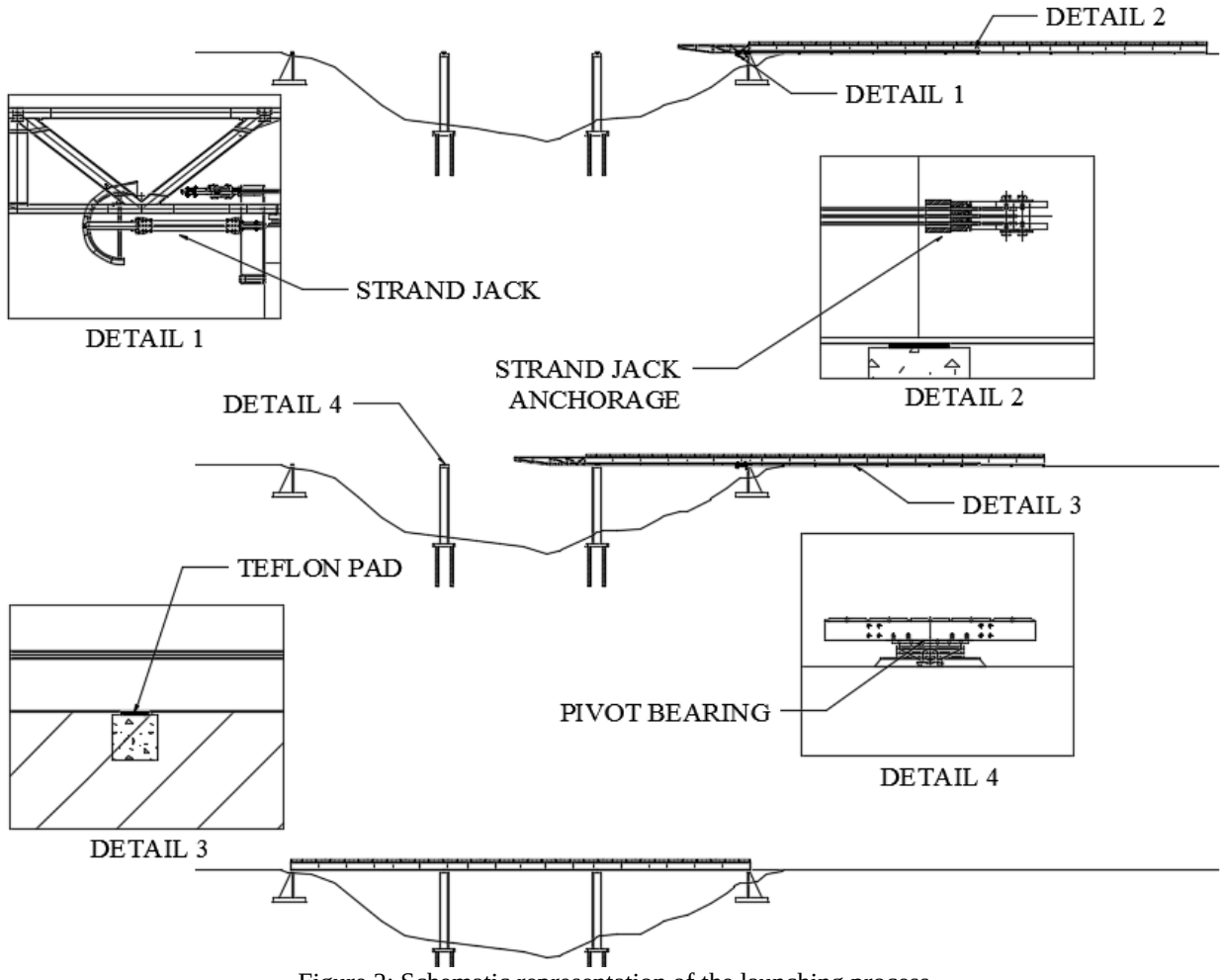

Figure 2: Schematic representation of the launching process

In the design stage of the Maresa Bridge, the structure was analyzed for the case where there is no launching nose attached to the girder ends. As discussed in Section 4, the results show that the strength of the structural components is sufficient to resist the effects of having the girders

cantilevering out 65m. In terms of deflections, the bridge structure could be erected at a higher level so the bottom flange at the cantilever end is supported by the pivot bearings when it reaches the piers or the abutment. The discussions presented in the next sections also consider that the structure is launched without nose to observe its behavior in the most demanding configuration, i.e., when the cantilever varies from 0m to 65m, while moving from Abutment "B" to Pier 2. As shown in later sections, the construction checks required by the AASHTO Specifications are conducted for different launching stages, at every 5m increments of the cantilever.

3. Finite Element Model Descriptions

The finite element analyses (FEA's) developed in this study are conducted in the ABAQUS v6.13 program (Simulia 2013). The structure is analyzed with two different types of modeling techniques. In the first group, girder webs are modeled with the S4R general purpose shell element. In this case, the girder webs are modeled with 20 shell elements. Flanges, transverse stiffeners, and longitudinal stiffeners are modeled with the B31 two-node beam element. Cross-frame top and bottom chords are modeled with B31 elements, and diagonals are modeled with the truss type element T3D2, from the ABAQUS library. The models developed with these characteristics are used to conduct elastic buckling analyses of the structure and to determine the construction required strength according to the applicable load combinations specified in the AASHTO LRFD Specifications. In particular, elastic geometric nonlinear analyses are developed to determine the load effects used to compute the required strength. Figure 3 shows the three-dimensional model of the Maresa Bridge developed in the ABAQUS program.

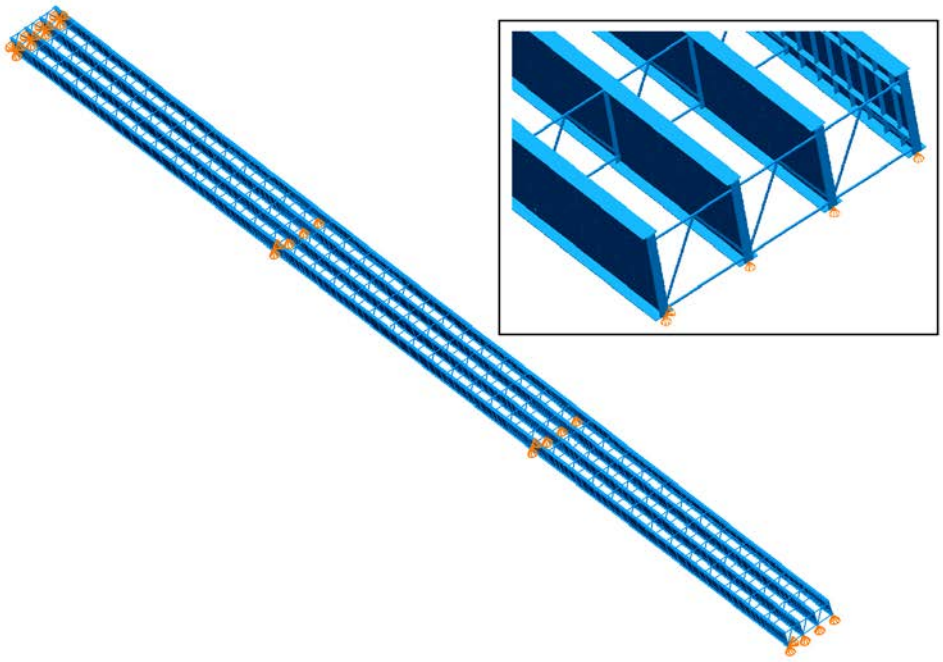

Figure 3: Three-dimensional representation of the Maresa Bridge used in the FEA

A second group of models is developed to conduct full nonlinear analyses of the case study. These types of analyses are developed in this research to obtain an accurate representation of the expected bridge behavior at different load levels. Full nonlinear analyses capture material and geometric nonlinearities and include also, the effects of residual stresses and geometric imperfections. The

characteristics of these models are the same as in the previous group, except that girder flanges are divided in ten parts across the width, and they are modeled with the same type of element used for modeling webs, i.e., S4R shell elements. Figure 4 shows the material model used in the analyses.

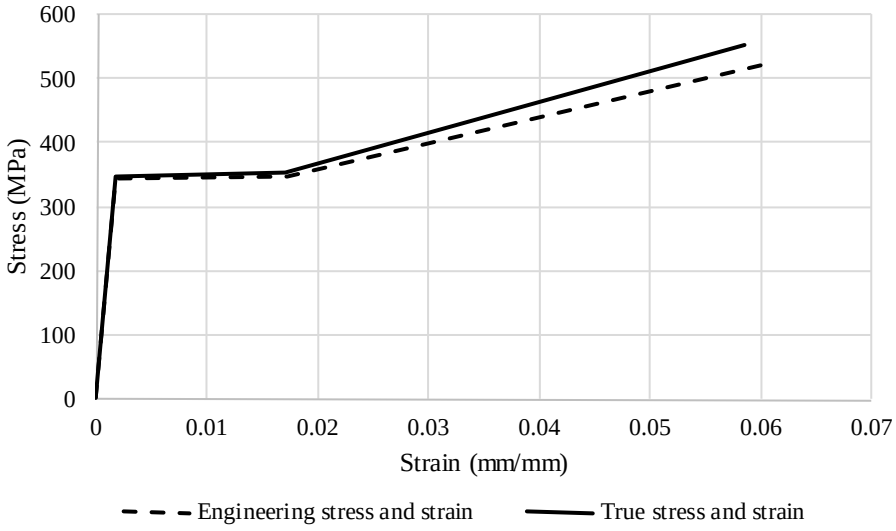

Figure 4: Stress – strain curve implemented in the FEA

Geometric imperfections are applied by first conducting a buckling analysis of the structure. Then, the deformed shape corresponding to the first buckling mode is scaled to a fraction of the acceptable deformation limits due to fabrication specified in AWS (2010). This reference provides limits for flange sweep, web out-of-straightness, and flange tilt. The residual stress pattern used in the models are based on measurements provided by Prawel et al. (1974). As shown in Kim (2010), FEA's conducted with this stress pattern provide accurate results as compared to those obtained from experimental tests on welded steel I-girders.

In this research, full nonlinear analyses are conducted by applying 50% of the values suggested by AWS (2010) and Prawel et al. (1974) for geometric imperfections and residual stresses, respectively. It is recommended to perform FEA's of built-up girders by applying this fraction of geometric imperfections and residual stresses, given the correlation that exists between experimental data and computer simulations (Subramanian and White 2015).

4. Construction Checks Required by the AASHTO LRFD Specifications for the Case Study

In this section, the results obtained from the FEM's are compared to the design strength values obtained from AASHTO (2014) for the Maresa bridge. This specification requires to conduct five different strength checks during construction for steel I-girders subject to flexure and shear. These are:

- Compression flange yielding $f_{bu} + f_{\ell} \le \phi_f R_h F_{yc}$
- Compression flange stability $f_{bu} + f_{\ell} / 3 \le \phi_f R_h F_{nc}$
- Web bend-buckling $f_{bu} \le \phi_f F_{crw}$
- Tension flange yielding $f_{bu} + f_{\ell} \le \phi_f R_h F_{yt}$

- Web shear strength $V_u \le \phi_v V_{cr}$

Also, to limit the levels of flange lateral bending, the specifications require the f_ℓ stresses not to exceed $0.6F_{yf}$.

In addition to the limit states shown above, for girder sections subject to concentrated loads applied to webs without bearing stiffeners, two other limit states are to be considered according to AASHTO (2014):

- Web local yielding $R_u \le \phi_b R_{ny}$
- Web crippling $R_u \le \phi_b R_{nc}$

In the context of the Maresa Bridge, as launching progresses, the girder panel at the cantilever support will be subject to a combination of all the limit states described above, i.e., bending, shear, and stresses due to point loads. As a result, this panel experiences the largest stresses in the structure. In fact, the largest strength requirements are observed when the cantilever approaches 65m, which is the span length.

To observe the behavior of a structure erected with ILM, the Maresa Bridge is studied using FEA. The launching process is simulated by increasing the cantilever 5m per step. For this purpose, in the FEM, the bridge supports are moved accordingly, so the structural responses are captured at each increment. Figure 5 depicts the deformed shape of the structure when the cantilever is equal to 55m, and it is subject to a gravity load equal to a factor times the self-weight. As presented in later sections, the factored load is equal to 2.57DC, and it is the collapse load for this structural condition. In the figure, the stress contour shows that the largest Von Mises stresses are located in the region near the cantilever support.

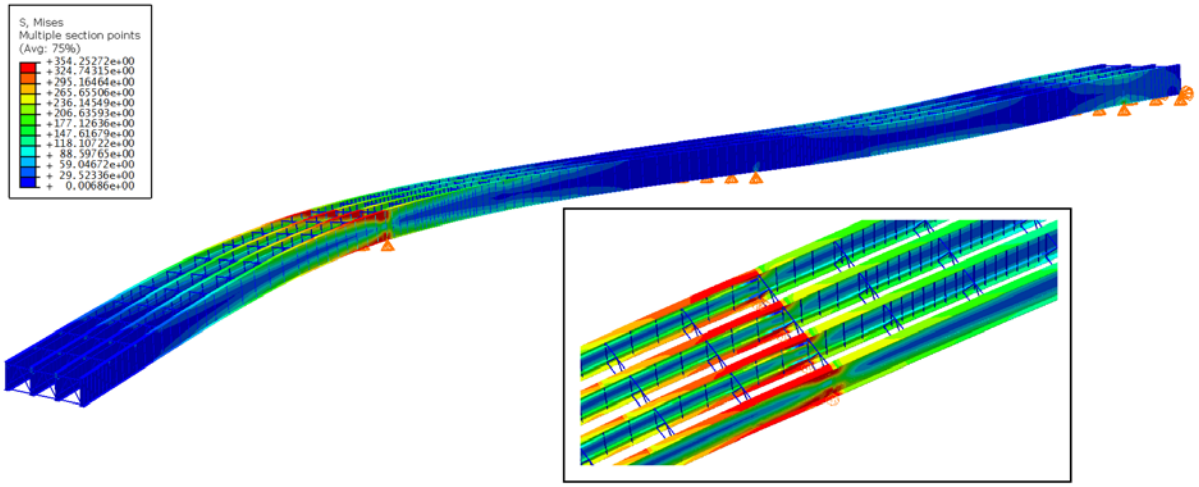

Figure 5: Illustration of the deformed structure as predicted by the FEM (stresses shown in MPa; deflections scaled by a x5 factor)

For the calculation of the strength checks described above, AASHTO (2014) requires to consider two types of loading: the structure's self-weight, DC, and the wind load acting on the superstructure, WS. The design wind velocity used for the calculation of WS is set to 50km/h, assuming that erection procedures will not take place at wind velocities higher than this value. These two types of loads are used to calculate the required strength for two load combinations:

Strength IV, 1.5DC, and the specific combination applied to construction, 1.25DC+1.25WS. These are the load combinations that need to be considered according to AASHTO (2014) for construction of steel girder bridges.

Figure 6 shows the plots corresponding to the strength checks for flexure and shear for the construction load combination and Strength IV. The plots include the design strength values for the corresponding limit states for girder G1 (i.e., an exterior girder) and also, the required strengths for the two load combinations mentioned before. The design strength calculations are based on the equations provided in the AASHTO Specifications. The stress values f_{bu} and f_{ℓ} used to compute the required strength in the load combinations are obtained from elastic geometric nonlinear analyses conducted with the characteristics discussed in the previous section.

In the plots, each pair of points represents the required and design strength for a given cantilever length at the cantilever support. For example, in Figure 6(b), the design strength of the girder at the cantilever support, for the compression flange stability limit state, when the cantilever is equal to 55m, is 324.68MPa. Similarly, the required strength of girder G1 for the same cantilever length, at the cantilever support, when considering the construction load combination is equal to 134.42MPa.

Since the objective of the paper is to study the behavior of steel bridges erected with ILM, the plots only include the results for the cantilever portions of G1 in the range of 35m to 65m. As shown in later sections, as the cantilever length increases, the interaction between flexure, shear, and local stresses due to point loads subject the steel girders to a combination of stresses that requires special considerations due to the high demands imposed near the cantilever support. For shorter cantilever lengths, the largest strength demands and controlling limit states do not occur near this region. Instead, they occur at regions controlled only by bending or shear (e.g., at the point of maximum moment, in the positive major-axis bending region), which are structural phenomena well understood by the bridge engineering profession and are well captured by current design provisions.

The plots show that for the Maresa Bridge, the strength checks are fulfilled at the girder panels near the cantilever support. In all the checks included in the plots, the girder section with the largest strength demands is at this location. As the cantilever increases from 35m to 65m, the different limit state checks are satisfied, showing that the structure complies with the AASHTO (2014) requirements for construction. The results of this study show that in terms of flexural and shear strength, this structure may be erected using ILM.

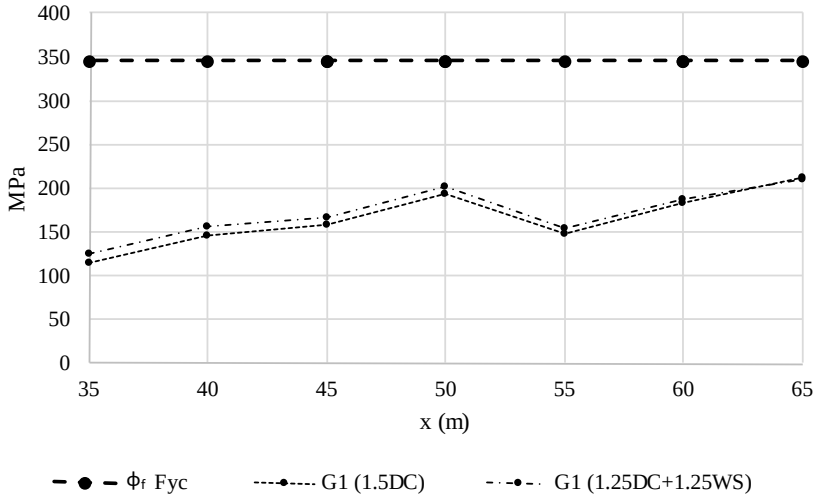

(a) Compression flange yielding

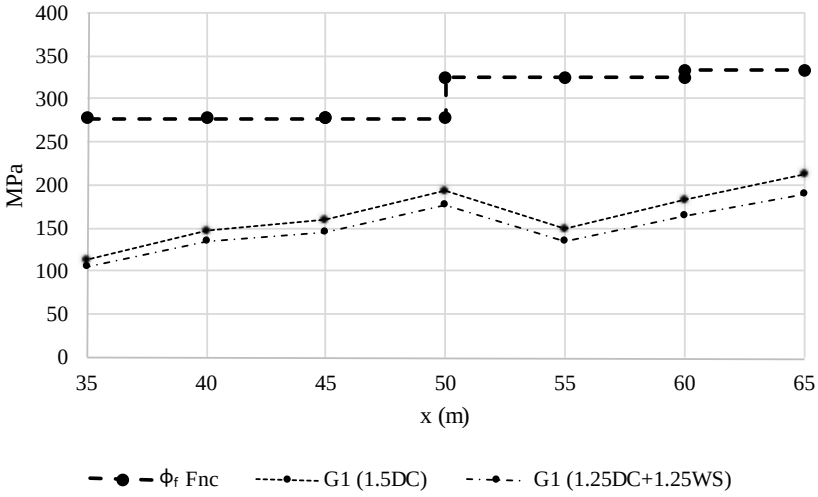

(b) Compression flange stability

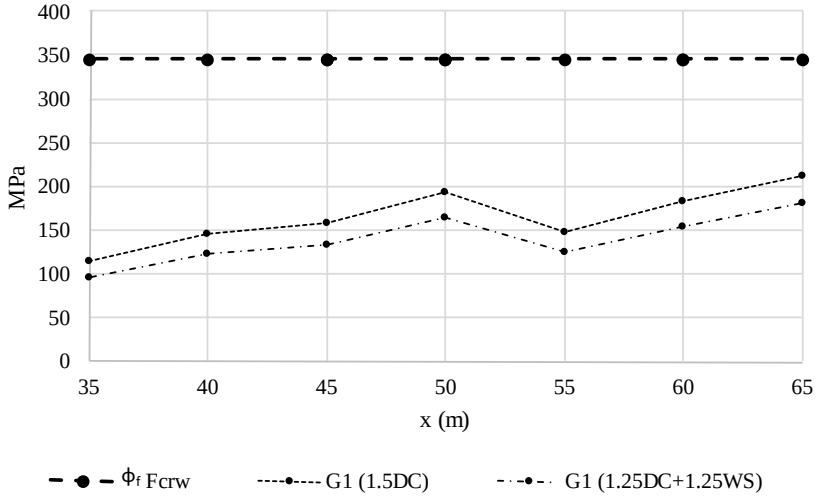

(c) Web bend-buckling resistance

Figure 6: AASHTO construction checks conducted for the Maresa Bridge during launching

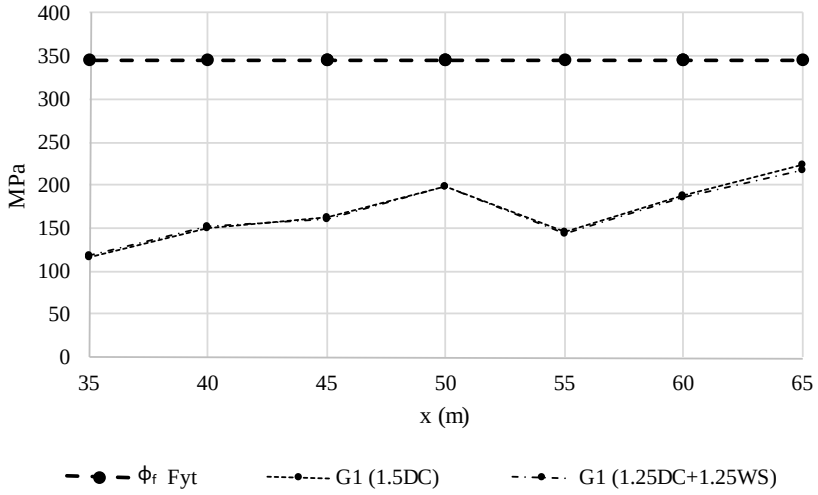

(d) Tension flange yielding

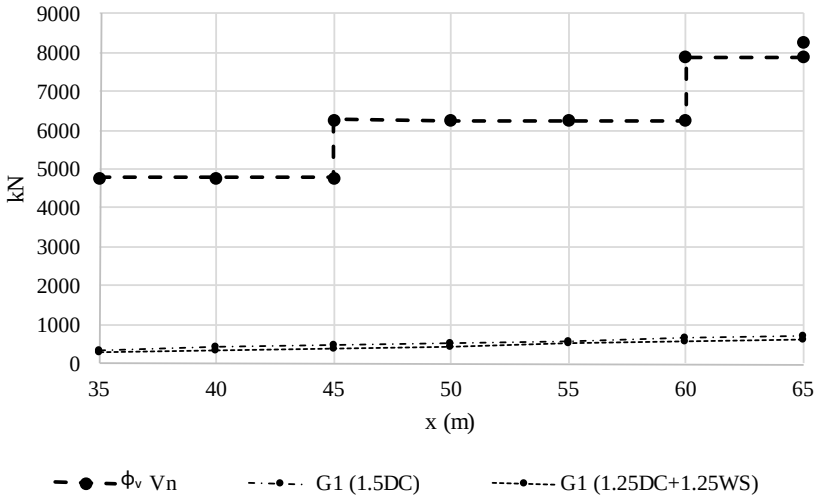

(e) Web shear strength

Figure 6: AASHTO construction checks conducted for the Maresa Bridge during launching (continued)

In addition to the limit states related to bending and shear, AASHTO (2014) requires to conduct strength checks at locations with concentrated loads applied to webs without bearing stiffeners. In particular, the specifications require to check the web strength for the limit states of web local yielding and web crippling. In the case of bridges erected with the ILM, as the girders cantilever out from the support (e.g., Abutment "B" in the Maresa Bridge), every point in the bottom flange is subject to a concentrated load. In steel I-girder bridges, bearing stiffeners are provided only at support locations. In the Maresa Bridge, for example, they are 65m apart, located at the abutments and piers. Therefore, for bridges in which ILM is selected as the erection method, girder webs must be checked for these two limit states.

Figure 7 shows a plot with these strength checks for the case study. The plot includes the design strength curves for the limit states of web crippling and web yielding. In addition, the required strength corresponding to the controlling Strength IV load combination is included for girder G1. The construction load combination is not included since it does not control over Strength IV, by

inspection. This plot is obtained following the same procedure described previously for the limit states of bending and shear.

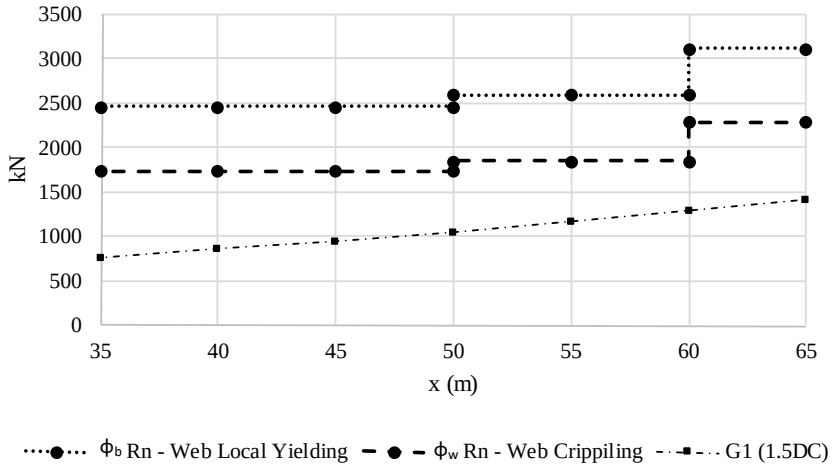

Figure 7: AASHTO construction checks due to point loads conducted for the Maresa Bridge during launching

As in the case of bending and shear, the plot in Figure 7 shows that the structure has sufficient strength to comply the specification requirements. Both the design strengths for web yielding and the web crippling are larger than the required strength, given by the Strength IV load combination.

The previous figures show that the case study satisfies the construction checks that are to be considered according to AASHTO (2014). All the limit states related to bending, shear, and point load effects are studied, showing that it is feasible to implement ILM for the erection of this structure.

5. Comparison between the AASHTO Specification Predictions and the Numerical Models at Ultimate Strength

One of the particularities of the AASHTO specifications is that each of the structural responses is checked separately. In the design philosophy of steel I-girders according to AASHTO (2014), flexure, shear, and point load effects are studied individually, i.e., the design equations do not consider interaction between these responses. Previous AASHTO design specifications used to include an interaction check for bending and shear (AASHTO 1998). However, correlation between experimental and substantial analytical research has demonstrated that bending and shear strength in steel I-girders are structural responses that are not necessarily interrelated and do not interact with each other (White et al. 2001, White et al. 2008, White 2008).

In bridges erected with ILM, in addition to these responses, there is a third stress component, given by the point load. For this reason, as depicted in Figure 5, the region adjacent to the cantilever support may be subject to high bending, high shear, and high point load effects. The presence of these three responses results in stress demands that requires special considerations. To determine the accuracy of the AASHTO design specifications, analyses are conducted on the case study using FEA. For this purpose, full nonlinear FEM's of the Maresa Bridge with the characteristics

described previously are developed, to study the maximum load carrying capacity of the structure and compare them to design strength predictions according to AASHTO (2014).

Figure 8 shows the AASHTO design strength predictions at the cantilever support, as well as the responses obtained from the FEA's for each of the six limits states previously detailed. The full nonlinear FEA's are conducted by increasing the loads for a load combination, e.g., 1.5DC, from zero up to the point of collapse. In the figures, the γ factors that multiply the load combinations indicate the maximum load carrying capacity of the structure. For example, when the cantilever is equal to 55m, the structure's capacity predicted by the FEA is 1.71 times the Strength IV load combination, or $1.71 \cdot 1.5DC = 2.57DC$. Similarly, for the construction load combination, the γ factor is 1.95, which results in 2.44DC+2.44WS.

As shown in these plots, for cantilever lengths of 50m and less, the design strength predicted with the AASHTO (2014) equations are conservative, as compared to the results obtained from the full nonlinear FEA's. In general, the design strength calculated according to the AASHTO specifications for the construction limit states is less than the analytical predictions. However, for longer cantilevers, the AASHTO (2014) design strength predictions are larger than the FEA predictions. For example, at a 55m cantilever length the design strength for the compression flange stability limit state is equal to 324.68MPa, while the stress value at maximum capacity is 253.00MPa for the case when there are only gravity loads applied to the system, and 261.93MPa for the case when there is a combination of gravity and lateral loads. For the other limit states, the observation made for the limit state of compression flange stability is the same. As the cantilever increases, the ability of the AASHTO predictions to capture the expected behavior becomes unconservative.

The results shown in these plots suggest that as the cantilever lengthens and the structural responses increase, there may be an interaction between bending, shear, and concentrated load stresses that current design methods are not capturing. The effects of the concentrated load at the support may need to be considered in combination with other structural responses. The analyses conducted in the case study indicate that further research is needed to comprehend the behavior of steel I-girder bridges erected with ILM and in general, of steel I-girders in cantilever.

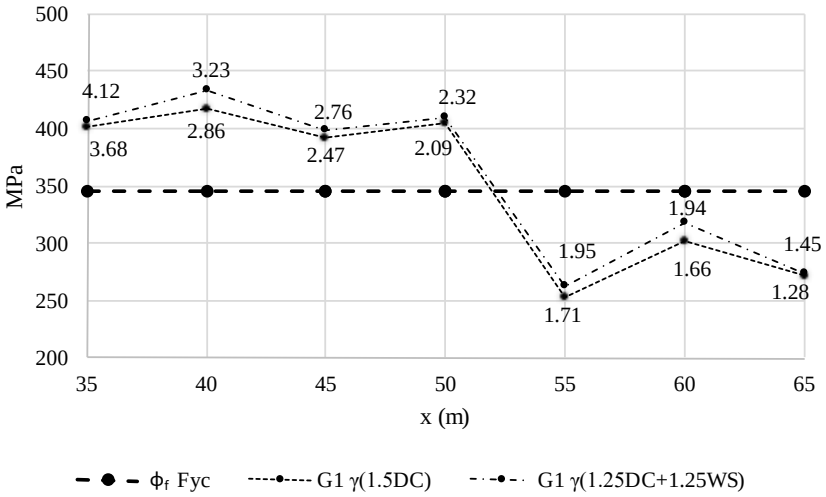

(a) Compression flange yielding

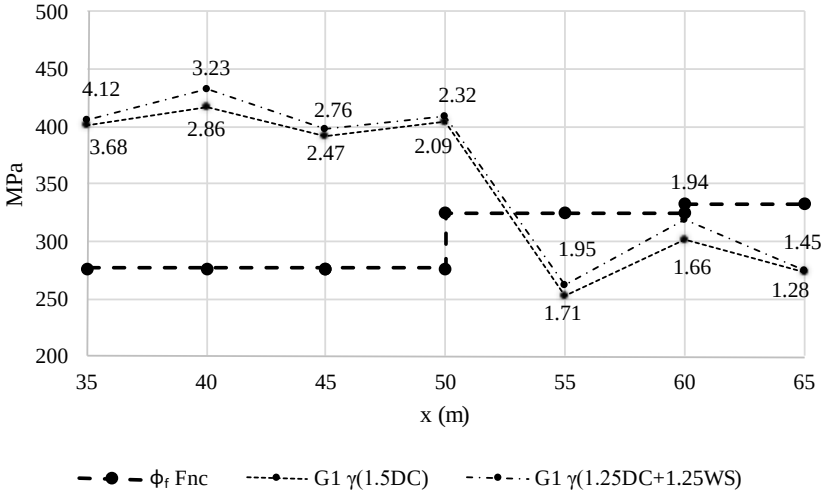

(b) Compression flange stability

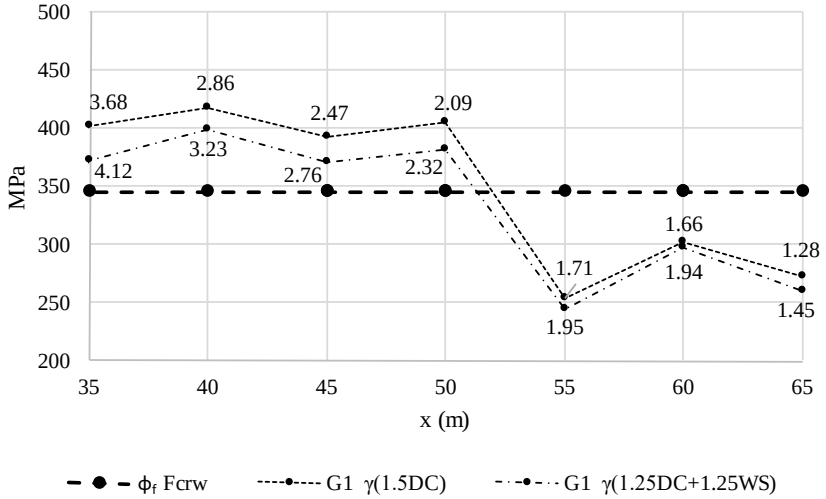

(c) Web bend-buckling resistance

Figure 8: Comparison between the AASHTO strength predictions and full nonlinear FEA results

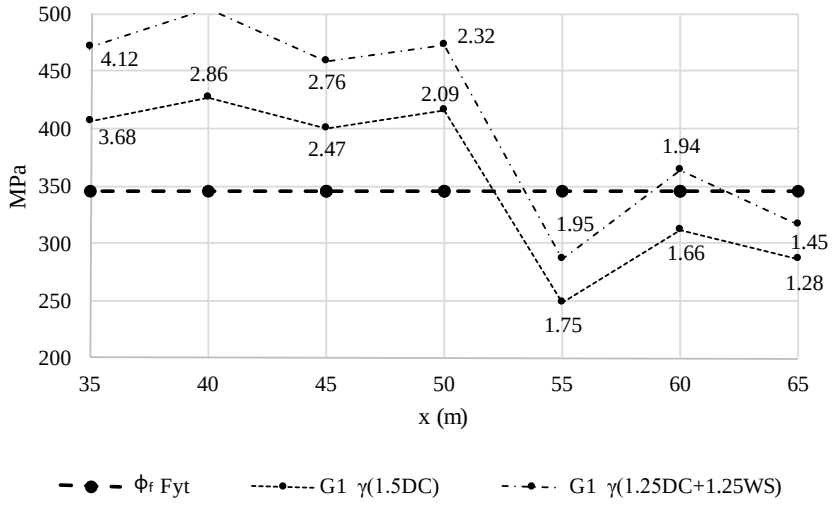

(d) Tension flange yielding

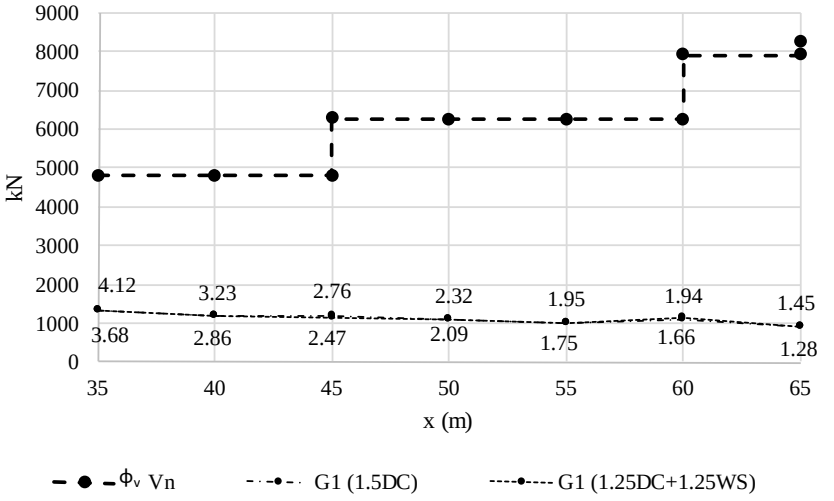

(e) Web shear strength

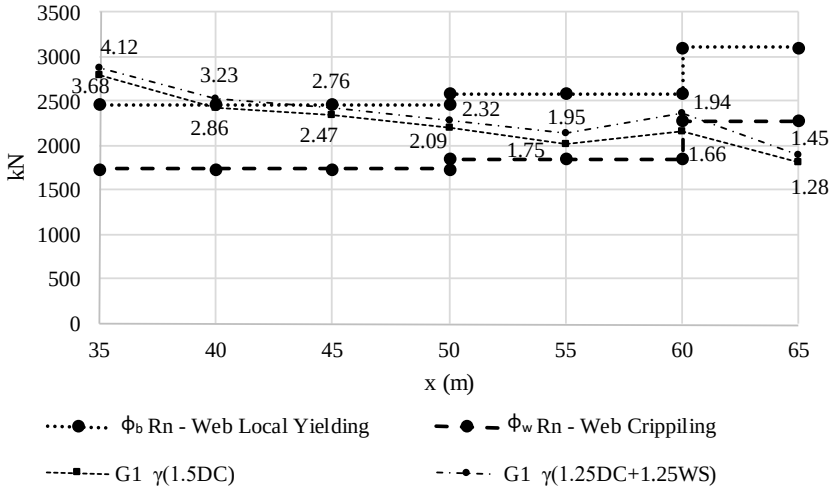

(f) Web crippling and yielding

Figure 8: Comparison between the AASHTO strength predictions and full nonlinear FEA results (continued)

6. System Global Buckling during ILM Operations

The limit states studied in previous sections relate to the structural behavior of individual girders. In addition to the analysis of the structural integrity of individual components, when ILM is used as the erection method, global buckling of the overall system should be considered. As the cantilever length increases during launching, so does the moment due to self-weight at the support, while the global lateral-torsional resistance of the system reduces. Therefore, this global limit state may control the strength of the system for long cantilevers.

To study the global lateral-torsional strength of bridges erected with ILM, the case study was modeled assuming that only two girders are erected at the time. Figure 9 depicts the first bucking mode obtained from the FEA for a cantilever equal to 65m. As shown for this case, overall global buckling may control over other structural stability phenomena.

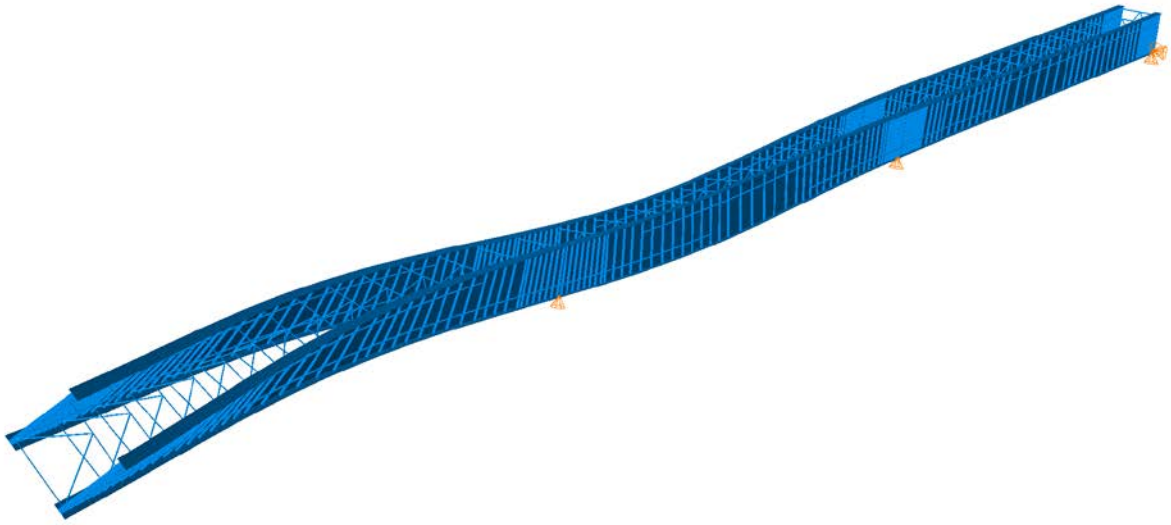

Figure 9: First buckling mode for the two girder system, cantilever = 65m

Structural instability due to global lateral-torsional buckling may be studied using the FEA techniques described in this paper. However, this is not always possible in practice, due to the specialized software needed to conduct the studies and the time invested to prepare the model. Yura et al (2008) developed the following closed form solution to predict the elastic global buckling strength for singly symmetric I-shaped girder systems:

$$M_{gl} = 2C_b \frac{\pi E}{L_g} \sqrt{\frac{I_{yc} J}{1.3} + \frac{\pi^2 I_{yc}^2 h_o^2}{L_g^2} + \frac{\pi^2 I_{eff} I_x S^2}{4 L_g^2}} \quad (1)$$

This equation predicts the resistance to global buckling for a twin-girder system such as the one depicted in Figure 9.

As discussed in the above reference, Eq. 1 has been validated for cases of uniform bending moment, while the effects of moment gradient are captured via C_b equations that are developed for single girders. In the context of bridges erected with ILM, C_b would correspond to the moment

gradient modifier for an overhang beam. For this case, AASHTO (2014) requires C_b to be equal to 1.0.

The results obtained with Eq. 1 and the FEA's are compared next, via the buckling factor, γ_{crt}. For the analytical solution, this factor is obtained by dividing M_{gl}, calculated with Eq. 1 by M_{u_gl}. The global required strength for flexure, M_{u_gl}, is computed as the moment at the cantilever support due to the structure's self-weight. For the FEA predictions, γ_{crt} is obtained directly from elastic buckling analyses.

Figure 10 shows γ_{crt} for the case study, with cantilever lengths between 50m and 65m. The plot includes the responses obtained from the FEA's with the actual girder geometry, i.e., considering the section changes (see Figure 1) and also, with a uniform girder section. For the latter case, the girder dimensions are D=2800mm, t_w=15mm, b_{fb}=600mm, t_{fb}=25mm, b_{ft}=470mm, and t_{ft}=25mm. These are the dimensions of the section with the smallest flange sizes in the girders, so the results obtained from analyses with these characteristics are expected to be conservative. The other two responses included in Figure 10 correspond to the predictions based on Eq. 1 with C_b=1.0 and C_b>1.0. This analytical solution does not capture the influence of girder section changes; therefore, the dimensions shown above are used in the calculations of M_{gl}, to obtain a conservative estimate.

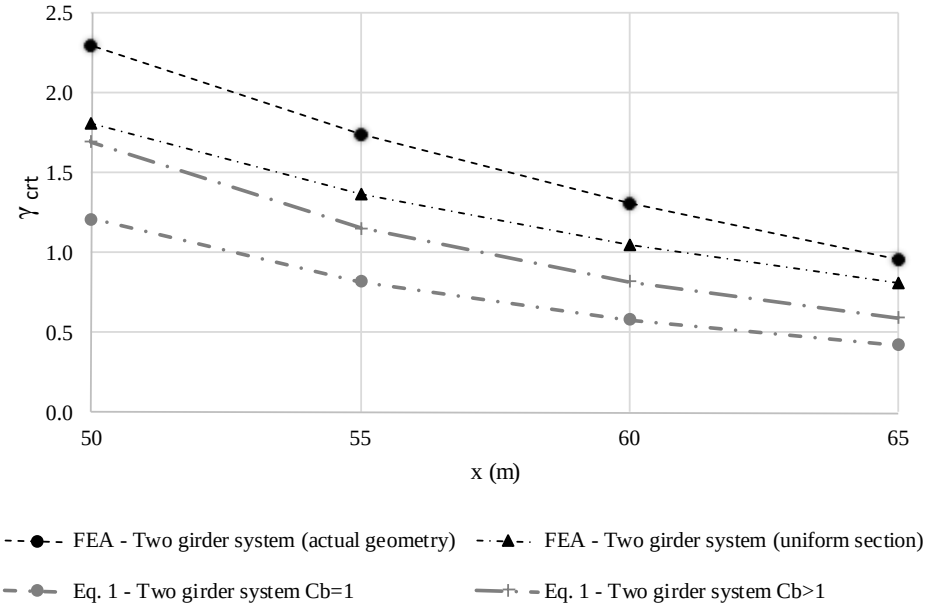

Figure 10: Comparison between FEA predictions and Yura et al (2008) predictions

The figure shows that the γ_{crt} predictions from the FEA's for the case with uniform girder section are smaller than those obtained for the actual geometry (i.e., including section changes). The FEA results for uniform girder section, however, serve as a reference to validate the predictions based on Eq. 1. As shown in the plot, there is an accurate correlation between the FEA's conducted with uniform section and the analytical responses. The values of γ_{crt} calculated with Eq. 1 and with and imposed value of C_b=1.4 are slightly lower than those obtained from the FEM with uniform section. This C_b value serves for illustration purposes only since it may vary for steel I-girder bridges with other dimensions. However, it is observed that the analytical solution with C_b=1.0

provides a conservative prediction of the expected response. Based on these observations, for preliminary design, it is recommended to investigate the global lateral-torsional buckling resistance using Eq. 1 and C_b=1.0. If γ_{crt} is less than 1.0, it is suggested to investigate the structure in more detail. For this purpose, a three-dimensional FEM of the bridge may be developed to obtain the elastic buckling modes and their associated γ_{crt} factors. Alternatively, Sanchez and White (2012) provide a methodology to assess the global buckling strength considering geometric nonlinear effects, based on Eq. 1 that may be used with C_b=1.0.

7. Summary and Conclusions

This paper presents the analyses conducted in a steel I-girder bridge to study the behavior of these types of structures when they are erected with ILM. The different construction limit states required by AASHTO (2014) for bridges constructed with this method are checked, showing that it is feasible to implement ILM for the case study.

The studies presented in this paper also show that for steel I-girder bridges erected with ILM, current AASHTO specifications may not predict the expected structural behavior at ultimate strength, as demonstrated by full nonlinear FEA results. The combination of high bending, high shear, and high patch loads subject the girder sections located near the cantilever support to stress concentrations that may not be properly captured with the design procedures of AASHTO (2014). Finally, studies conducted to observe the global lateral-torsional buckling resistance of the case study show that for bridges erected with ILM, this response may control over the limit states considered for individual girders. The equation proposed by Yura et al (2008) correlates well with the results obtained from the FEA's for different cantilever lengths, and it is conservative if the moment gradient modifier is set to C_b=1.

8. Future Work

The results discussed in the previous sections show that further studies are required to better comprehend the correlation between bending, shear, and concentrated loads. Previous research has evidenced that in steel I-girders, bending and shear are structural phenomena that do not necessarily interact with each other. However, in cases such as bridges erected with ILM, there is an additional component, i.e., concentrated loads, that may have a significant effect in the strength of I-girders. In this context, further studies are needed to understand the potential interaction between these three structural responses and their effects in the behavior of these structures.

In the case of the global lateral-torsional buckling predictions, Eq. 1 with C_b=1 provides a simple and conservative method to investigate this limit state. However, further studies are needed to develop or implement existing methods for the calculation of C_b in twin-girder systems in cantilever. The authors will conduct further research on these topics, which will be presented in future papers.

Acknowledgements

The research presented in this paper is part of the construction engineering studies conducted for RIPCONCIV Cia. Ltda. and KUBIEC-CONDUIT S.A. The authors would like to acknowledge the financial support of these organizations. The opinions, findings, and conclusions expressed in this paper are the authors' and do not necessarily reflect the views of the above organizations.

References

AASHTO (1998). AASHTO LRFD Bridge Design Specifications. 2nd Edition, American Association of State Highway and Transportation Officials, Washington, DC.

AASHTO (2014). AASHTO LRFD Bridge Design Specifications. 7th Edition, American Association of State Highway and Transportation Officials, Washington, DC.

AWS (2010). Structural Welding Code – Steel, AWS D1.1M, 22nd ed., prepared by the AWS Committee on Structural Welding, 572 oo.

Kim, Y. D. (2010). "Behavior and Design of Metal Building Frames Using General Prismatic and Web-Tapered Steel I-Section Members." Doctoral Dissertation, School of Civil and Environmental Engineering, Georgia Institute of Technology, Atlanta, GA, 562pp.

LaViolette, M., Wipf, T., Lee, Y., Bigelow, J., and Phares, B. (2007). "Bridge Construction Practices Using Incremental Launching." American Association of State Highway and Transportation Officials, Washington, DC.

Prawel, S. P., Morrell, M. L., and Lee, G. C. (1974). "Bending and Buckling Strength of Tapered Structural Members." Welding Research Supplement, Vol. 53, February, 75-84.

Sanchez, T. A., White, D. W. (2012). "Stability of Curved Steel I-Girder Bridges During Construction." Transportation Research Record: Journal of the Transportation Research Board, Transportation Research Board, Washington, D.C., Vol. 2268, 122-129.

Simulia (2013). ABAQUS/Standard Version 6.13, Dassault Systèmes, Inc. Providence, RI, http://www.3ds.com/products-services/simulia/products/abaqus/

Subramanian, L., White, D.W. (2015). "Evaluation of Lateral Torsional Buckling Resistance Equations in AISC and AASHTO." Proceedings of the Annual Stability Conference, Structural Stability Research Council, Nashville, TN, 20pp.

White, D. W., Zureick, A. H., Phoawanich, N., and Jung, S.-K. (2001). "Development of Unified Equations for Design of Curved and Straight Steel Bridge I-Girders." Final Report to American Iron and Steel Institute Transportation and Infrastructure Committee, Professional Services Industries, Inc., and Federal Highway Administration, School of Civil and Environmental Engineering, Georgia Institute of Technology, Atlanta, GA.

White, D. W., Barker, M. G., Azizinamini, A. (2008). "Shear Strength and Moment-Shear Interaction in Transversely Stiffened Steel I-Girder." Journal of Structural Engineering, American Society of Civil Engineers, Reston, VA, Vol. 134, No. 9, 1437-1449.

White, D. W. (2008). "Unified Flexural Resistance Equations for Stability Design of Steel I-Section Members – Overview." Journal of Structural Engineering, American Society of Civil Engineers, Reston, VA, Vol. 134, No. 9, 1405-1424.

Yura, J., Helwig, T., Herman, R., and Zhou, C. (2008). "Global Lateral Bucklin of I-Shaped Girder Systems." Journal of Structural Engineering, American Society of Civil Engineers, Reston, VA, Vol. 134, No. 9, 1487-1494.